BIOTROPICA *(*): ***–*** ****   10.1111/j.1744-7429.2007.00353.x

Amazon Forest Structure from IKONOS Satellite Data and the Automated Characterization of Forest Canopy Properties

Michael Palace[1,4], **Michael Keller**[1,2], **Gregory P. Asner**[3], **Stephen Hagen**[1], and **Bobby Braswell**[1]

[1]Complex Systems Research Center, Morse Hall, University of New Hampshire, Durham, New Hampshire 03824, U.S.A.

[2]International Institute of Tropical Forestry, USDA Forest Service, Rio Piedras, Porto Rico 00928–5000 U.S.A., CENA/USP, Av. Centenário, 303, P.O. Box 96 Piracicaba, CEP 13400–970, SP, Brazil

[3]Department of Global Ecology, Carnegie Institution, Stanford, California 94305, U.S.A.

ABSTRACT

We developed an automated tree crown analysis algorithm using 1-m panchromatic IKONOS satellite images to examine forest canopy structure in the Brazilian Amazon. The algorithm was calibrated on the landscape level with tree geometry and forest stand data at the Fazenda Cauaxi (3.75° S, 48.37° W) in the eastern Amazon, and then compared with forest stand data at Tapajos National Forest (3.08° S, 54.94° W) in the central Amazon. The average remotely sensed crown width (mean ± SE) was 12.7 ± 0.1 m (range: 2.0–34.0 m) and frequency of trees was 76.6 trees/ha at Cauaxi. At Tapajos, remotely sensed crown width was 13.1 ± 0.1 m (range: 2.0–38.0 m) and frequency of trees was 76.4 trees/ha. At both Cauaxi and Tapajos, the remotely sensed average crown widths were within 3 percent of the crown widths derived from field measurements, although crown distributions showed significant differences between field-measured and automated methods. We used the remote sensing algorithm to estimate crown dimensions and forest structural properties in 51 forest stands (1 km^2) throughout the Brazilian Amazon. The estimated crown widths, tree diameters (dbh), and stem frequencies differed widely among sites, while estimated biomass was similar among most sites. Sources of observed errors included an inability to detect understory crowns and to separate adjacent, intermingled crowns. Nonetheless, our technique can serve to provide information about structural characteristics of large areas of unsurveyed forest throughout Amazonia.

Key words: Amazonia; automated algorithm; biomass; crown delineation; crown width; rain forest; tropical forest.

Tropical forests are structurally complex ecosystems (Whitmore 1982). Components of forest structure include canopy geometry, tree architecture, size distributions of trees, areal tree density, and biomass (Spies 1998). Tropical forests are marked by high biological diversity and complex vegetation dynamics that result in a spatially diverse array of forest structures (Richards 1952, Denslow 1980, Salati & Vose 1984, Terborgh 1992, Terborgh *et al.* 1996, Ozanne *et al.* 2003). Knowledge of the forest structure in tropical forests in general and in the Amazon region in particular is vital for the estimation of carbon stocks and fluxes in global budgets (Houghton *et al.* 2000, 2001), habitat and faunal distributions (Schwarzkopt & Rylands 1989), and interactions between the biosphere and atmosphere (Keller *et al.* 2004).

The height and architectural complexity of the canopy, along with the logistical challenges of tropical field research and methodologies, limit studies of tropical forest structure. In some areas, such as the Amazon Basin, permanent plots that can be used for quantification of forest structure are relatively few and poorly distributed spatially (Malhi *et al.* 2006). Remote sensing can supplement traditional ecological studies by providing observations of large areas (Roughgarden *et al.* 1991, Shugart *et al.* 2001).

A series of Landsat sensors have provided the data most often used in remote sensing studies of vegetation cover in the humid tropics (Roberts *et al.* 2003). The spatial resolution (∼30 m) and spectral coverage (seven bands) of Landsat data allow identification of broad land-cover features and changes such as deforestation (*e.g.*, Skole & Tucker 1993). More subtle changes resulting from logging can be discerned in spectral mixture model analysis of Landsat and similar data (Souza *et al.* 2003, Asner *et al.* 2005). However, extraction of tropical forest structural properties from Landsat data is challenging because the image resolution is comparable to the size of the largest tree crowns (Moran *et al.* 1994; Steininger 1996, Scarth & Phinn 2000).

An alternative approach to the remote sensing of forest structure is the delineation of individual crowns using high spatial resolution data smaller then the average crown width (Culvenor 2002, Pouliot *et al.* 2002, Read *et al.* 2003, Leckie *et al.* 2003b). Photographic imagery has been used for the estimation of stand density and crown widths (Dawkins 1962, Larsen & Rudemo 1998, Bolduc *et al.* 1999, Fensham *et al.* 2002, Popescu *et al.* 2003, Falkowski *et al.* 2006). Videography has also been used along transects to analyze forest structural components, including individual crowns (Culvenor 2002, Brown *et al.* 2005). Lidar (light detection and ranging data) sensors flown on aircraft have also been used in the crown delineation (Popescu *et al.* 2003, Leckie *et al.* 2003a, Falkowski *et al.* 2006).

Satellite imagery has been used for crown delineation using visual interpretation or automated methods (Gougeon 1995a,b; Wulder *et al.* 2000; Culvenor 2002; Pouliot *et al.* 2002; Leckie *et al.* 2005a,b). Visual interpretation approaches are resource intensive and difficult to implement consistently (Asner *et al.* 2002), whereas existing automated routines can be readily replicated but also may be inaccurate (Culvenor 2002). Newer satellite instruments, such

Received 16 March 2007; revision accepted 24 May 2007.
[4] Corresponding author; e-mail: michael.palace@unh.edu

as IKONOS and Quickbird, provide relatively inexpensive high spatial resolution images for remote areas. These high spatial resolution satellite image data have been used to estimate the number of trees per area, individual crowns widths, and gap structure in tropical forests (Asner *et al.* 2002, Read *et al.* 2003, Clark *et al.* 2004). Previous studies have covered small geographic areas (< 10 km^2) because of the labor involved in manual methods of image analysis.

There are a variety of automated pattern recognition methods that are used to isolate individual trees and vegetation structure from high spatial resolution data, including semi-variograms, wavelet analysis, image segmentation, local maxima finding and filtering, template matching, valley finding, 3D modeling, and space-scale theory (Gougeon 1995a, Brandtberg & Walter 1998, Quackenbush *et al*. 2000, Stiteler & Hopkins 2000, Wulder *et al.* 2000, Shugart *et al.* 2001, Gong *et al.* 2002, Pouliot *et al.* 2002, Weinacker *et al.* 2004, Popescu *et al.* 2003, Leckie *et al.* 2003a,b, Caelli *et al*. 2005, Chen *et al.* 2006, Cheng *et al*. 2006, Chubey *et al.* 2006, Falkowski *et al.* 2006, Jensen & Sanchez Azofeifa 2006). The two more commonly used algorithms for automated analysis of canopies using high spatial resolution panchromatic passive optical data are: (1) local maximum filtering, and (2) local minima value finding. Local maximum filtering has proven accurate in estimation of the number of trees per unit area (Wulder *et al.* 2000). This method assumes that the area surrounding the brightest local value can be associated with the location of a single tree crown or the crown apex (Wulder *et al.* 2000, Culvenor 2002). Local minima value finding has been used to detect the separation between two crowns, assuming that the darker image values are created by shadows between crowns and valleys between canopy apexes (Pouliot *et al.* 2002, Leckie *et al.* 2003b). Automated crown detection algorithms using a combination of local maximum filtering and local minima value finding have been developed (Pouliot *et al.* 2002, Leckie *et al.* 2003b) but they have not yet been applied to tropical forests.

In addition to panchromatic data, high spatial resolution multi-spectral and lidar data have been used for crown delineation and are often collected and analyzed in conjunction. These methods also primarily rely on local maximum and local minima value finding methods, with additional filtering or enhancement methods, such as wavelet-based segmentation (Gougeon 1995a, Popescu *et al.* 2003, Leckie *et al.* 2003b, Falkowski *et al.* 2006). Currently, high spatial resolution multi-spectral and lidar imagery collected from airplanes is scarce and expensive.

Current work involving crown geometry and high-resolution imagery has focused on analysis of temperate forests, boreal forests, and plantations (Larsen & Rudemo 1998, Culvenor 2002, Pouliot *et al.* 2002, Popescu *et al.* 2003, Leckie *et al.* 2003a,b, Falkowski *et al.* 2006). There is a strong bias toward systems with low species diversity and relatively regular geometric crown shapes (especially conifer forests) facilitating automated crown detection. In contrast, tropical broadleaf forests have high species diversity and highly diverse and irregular crown geometries. We present an automated crown delineation algorithm based on existing pattern recognition concepts, to perform the first automated crown delineation from IKONOS satellite images collected over tropical forests in Brazil.

Because accurate geolocation is extremely difficult in the dense understory of tropical forests, we did not examine crown location on a tree-by-tree basis. Instead, we compared the remotely sensed measurements of stem frequency and canopy width to field surveys at two forest sites in the central and eastern Amazon on a stand basis, and we also used allometric equations to extend the remote sensing estimates to distributions of diameter at breast height (dbh) and biomass. We applied the detection algorithm and allometric equations to 51 forest stands from IKONOS images spread throughout the Brazilian Amazon to estimate crown dimensions and biomass across a range of mature forest conditions.

METHODS

SATELLITE IMAGERY.—We used seven IKONOS satellite images (Space Imaging Inc., Thorton, CO, U.S.A.) collected throughout the Brazilian Amazon. The 1-m panchromatic data were acquired through the Large-Scale Biosphere-Atmosphere Experiment in Amazonia (LBA) project (Hurtt *et al.* 2003, Keller *et al.* 2004; http://eos-webster.sr.unh.edu/home.jsp). The IKONOS images were subset to 53 1-km^2 areas containing intact, closed-canopy forest for subsequent analysis using our crown detection and analysis algorithm (Table S1). Two of these areas, Cauaxi and Tapajos, were used to develop our automated crown detection algorithm, through comparisons with field data. We characterized forest canopy properties on the remaining 51 areas, and the results were compared for differences in forest structure. Geographical coordinates for these 51 areas are presented in Table S1. No cross-validation was conducted because we only measured crown widths in the field at Cauaxi.

CROWN DETECTION AND ANALYSIS.—Our automated crown detection algorithm was designed using existing pattern recognition concepts with high spatial resolution remote sensing data, such as from IKONOS and similar spaceborne sensors. The algorithm is based on spatial analysis of the brightness patterns in the image (visible reflectance, digital number (DN)). This algorithm, developed using Matlab and Visual Basic, combines local maximum filtering and local minima value-finding methods, with analysis of ordinal transect data radiating outward from a crown apex (local maximum) (Culvenor 2002, Pouliot *et al.* 2002). There are two preprocessing steps. First, the modal, maximum, and minimum brightness value of each IKONOS image is calculated. These statistics are used to set the dynamic range of an iterative, local-maximum finding step, as explained later. The overall image contrast and brightness affects how the algorithm processes iterative local maxima. We set the limit to half the dynamic range based on our calibration of the Cauaxi image. During that calibration we found that the smallest local maximum value was nearly equal to the modal brightness value for the entire image. Since our intention is to develop a fully automated crown characterization algorithm, we used the modal brightness value of the image to set the limit for the lowest iterative local maximum.

Our second preprocessing step involves a 3×3 pixel moving window averaging filter used to smooth the image, a method commonly used in pattern recognition. Based on preliminary work we found more consistent results when such an averaging filter was applied. The moving window filter retains information on a 1 × 1 m pixel resolution by averaging the value of each pixel and its eight adjacent neighbors. After application of the filter, each pixel still retains a unique value and the 1-m image resolution is retained. The moving window averaging filter was applied because the large dynamic range of IKONOS image data (11-bit) resolution results in high levels of pixel-to-pixel variability.

After preprocessing, local maximum brightness values are identified by searching the entire image for the highest brightness value. The local maximum seeds an ordinal transect analysis described later. Once all local maxima of a specific brightness value are analyzed throughout the image, the algorithm proceeds to the next lower brightness value and iterates the local maximum finding and crown delineation process. This iterative process continues until the local maximum reaches the limit of the modal brightness value of the image, determined in the preprocessing stage of analysis.

After a local maximum is selected, image brightness values are analyzed in 360 directions (ordinates) from each local maximum or nodal pixel as a transect (linear series of pixels). Use of the ordinal transect analyzes an area around the local maximum allowing for a variable size window in the analysis of the crown dimensions. Though 360 directions are not needed in smaller crown analysis, we found it was useful for larger crowns. With a one degree separation of ordinal transects, adjacent ordinal transects begin to analyze different pixels at 29 pixels from the local maximum. Use of 360 ordinal directions also makes this algorithm directly applicable to images with higher spatial resolution such as airborne lidar and aerial photography.

An individual ordinal transect is terminated when the observed digital number (DN) value between the current pixel and the adjacent pixel on the transect increases by more than a threshold value that we call the derivative threshold (Fig. 1). The ordinate length is limited to 40 m based on maximum crown dimensions observed in the field. The derivative threshold was fixed based on a sensitivity analysis described below. We recognize that any given ordinal transect may end prematurely because of shadows. Or alternatively, a given ordinal transect may extend beyond an individual crown because of merged crowns or because lianas bridge adjacent crowns.

Although our algorithm does not have a variable window size for each local maximum, our iterative approach to the search for local maxima effectively implements variable window sizes. During the first iteration of the search, the highest DN values are selected. Because the ordinal transect continues in 360 directions and up to 40 pixels in any direction, the initial window size is a 40-pixel radius. After the identification of crowns at a specific DN value, pixels identified as crowns are removed from future searches for local maximum and are also removed from the searches along ordinal transects. Therefore, following the highest DN values, window size tends to shrink. This approach is adaptive because it responds to image characteristics and forest structure and does not require site-based parameterization necessary for most variable window size methods.

In the development of our algorithm we examined whether the ordinal transect length was biased in any one direction. To examine such a bias we binned ordinal transect into eight groups of 45 degrees and applied an ANOVA. We performed multiple comparisons using Tukey's HSD tests for both the Cauaxi and Tapajos images. At Cauaxi, ordinal transect directions were significantly different from one another ($F = 1106$) except direction 46–90° and 136–180°, which were indistinguishable (Fig. 2A). At Tapajos, the ANOVA also indicated differences among ordinal transect directions overall ($F = 800$, $P < 0.0001$); however, the bias in largest ordinal length directions were different than at Cauxi. Using data sets that included the IKONOS images we examine here, Asner and Warner (2003) found that view geometry and solar zenith and azimuth angles had no apparent influence on the shadow fraction in IKONOS imagery. These findings suggest no strong effect of a directional bias.

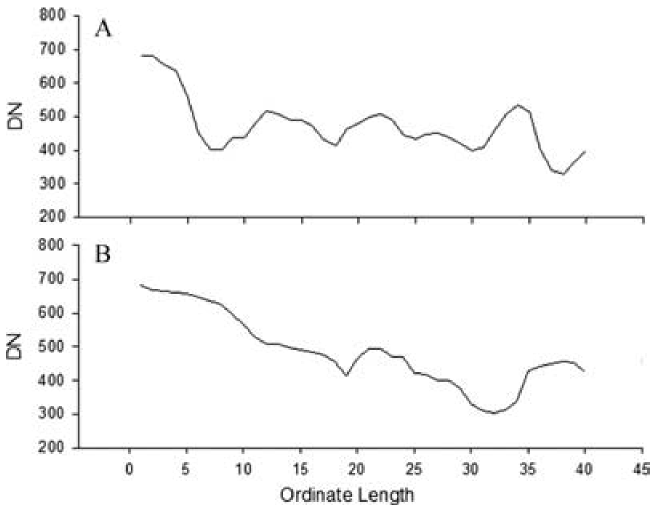

FIGURE 1. Digital number data used for termination of an ordinate for two selected ordinal transects at Cauxi. (A) The crown edge is estimated to be 8 pixels from the local maxima. (B) The crown edge is estimated to be 20 pixels from local maxima.

For simplicity, tree crowns were approximated as circles centered on the local maximum, based on the assumption that an undamaged tree has branches that radiate evenly out from the central stem or trunk (Brandtberg & Walker 1998). The crown is represented by a circle with a radius that is half the sum of the longest pair of opposing ordinal transects (Fig. 2B). After a crown is located and delineated, the pixels within the crown area are removed from further analysis. No new ordinal transects are extended into an existing crown, and remaining local maxima within delineated crowns are not analyzed. Crowns may overlap when ordinal transects from a neighboring tree generate a sufficiently large crown width for two circular canopies to overlap.

FIELD DATA AND ALLOMETRIC EQUATIONS.—We did not attempt to compare locations of individual trees between field and image data. In a previous study at La Selva, Costa Rica, Read *et al.* (2003) found that it was extremely difficult to acquire submeter locations using a Global Positioning System (GPS) receiver even for large emergent trees. Location of individual canopies is complicated because of

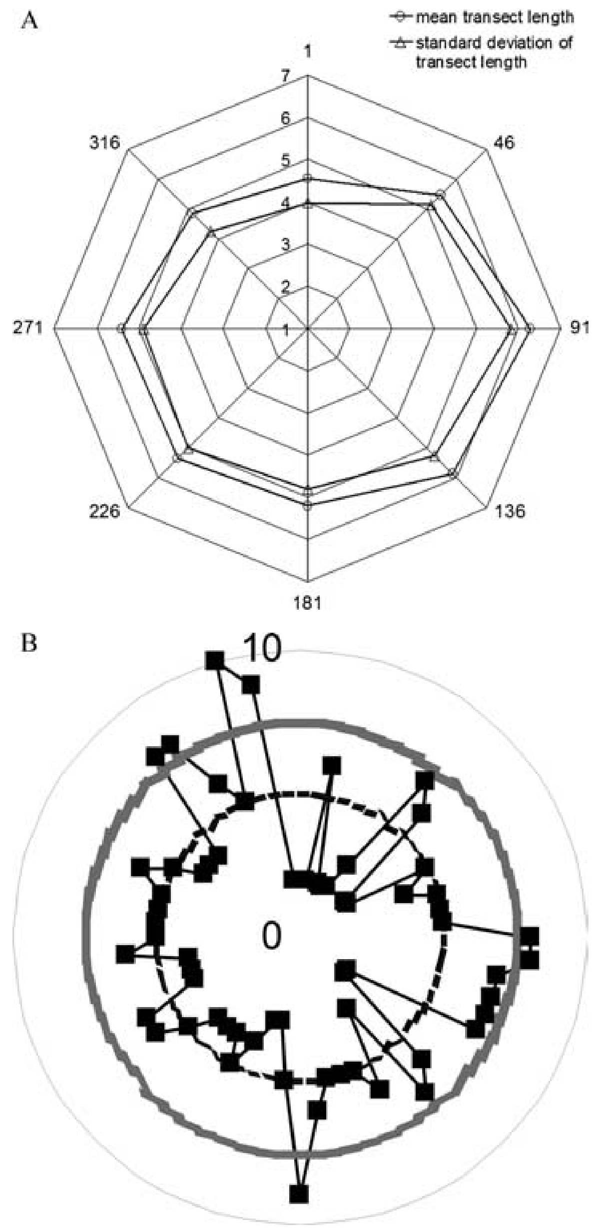

FIGURE 2. (A) Mean and standard deviation binned ordinal transects ($N = 484{,}200$) from crowns analyzed at Cauaxi. Distances in meters with directions in degrees relative to true north. The original 360 ordinal transect were binned into eight directions. (B) An example of ordinal transects used in automated crown detection showing 64 ordinal transects. Ordinal lengths are connected by lines purely for presentational purposes. The dotted circle is the estimated crown using a radius of half the sum of the two longest opposing ordinal transects. The solid gray circle is the average of all transects. A 10 m radius circle is depicted by the largest circle.

geo-rectification errors related to topography and ground-truthed reference points. More importantly, the dense vegetation of the tropical forest makes it difficult to acquire GPS signals with sufficient accuracy for meter-scale location. We focus on a statistical representation of the canopy as opposed to a crown-by-crown identification.

Field data on crown dimensions are extremely scarce for Amazon forests. We collected measurements of crown width, depth, tree height, and dbh for ~300 trees in a 50-ha stand on the Fazenda Cauaxi in the eastern Brazilian Amazon (Asner *et al.* 2002). Crown position (understory or canopy) and dbh were also measured for > 2700 trees using a stratified sampling methodology (Asner *et al.* 2002). We relied on these measurements to test and calibrate our remote sensing algorithm. Additional stand data for the Tapajos National Forest in the central Brazilian Amazon were provided by Keller *et al.* (2001) (392 ha) and Rice *et al.* (2004) (20 ha) to test the algorithm in a second forest stand.

For the estimation of aboveground biomass and carbon stocks in tropical forests, allometric equations for trees utilize dbh, tree height, or both (*e.g.*, Brown 1997, Chave *et al.* 2005). However, optical remotely sensing data from IKONOS cannot be used to directly measure either height or dbh for trees in closed canopies. Therefore, allometric equations based on crown diameter were needed. We developed a relation ($R^2 = 0.57$, $P < 0.0001$) between crown width (m) and dbh (cm) from 300 individual trees as discussed above:

$$\text{dbh} = 0.0381 \times (\text{crown width})^2 + 2.33 \times (\text{crown width}) + 15.5. \quad (1)$$

A commonly used allometric equation for tropical forests developed by Brown (1997) was then used to extend the remote sensing observations of crown width to biomass (kg dry matter) via dbh:

$$\text{Biomass} = (42.69 - 12.80 \times \text{dbh} + 1.242 \times \text{dbh}^2)/1000. \quad (2)$$

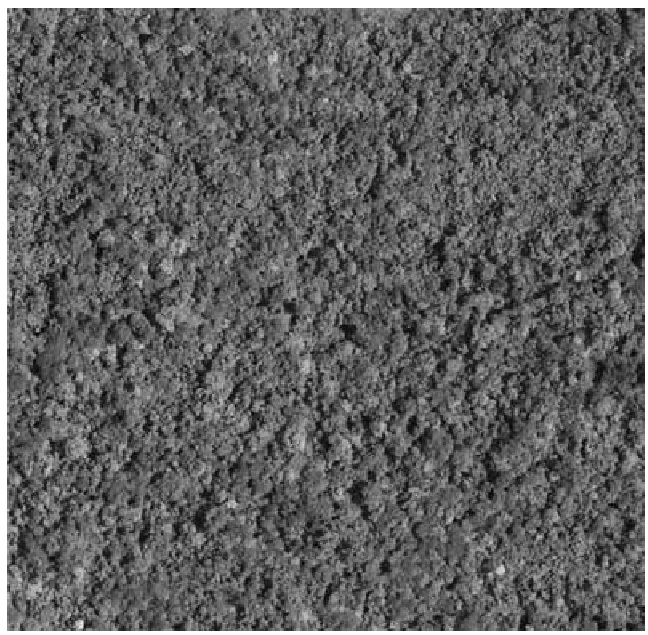

FIGURE 3. IKONOS image of the 64-ha area on the Fazenda Cauaxi used for calibration of the crown detection algorithm.

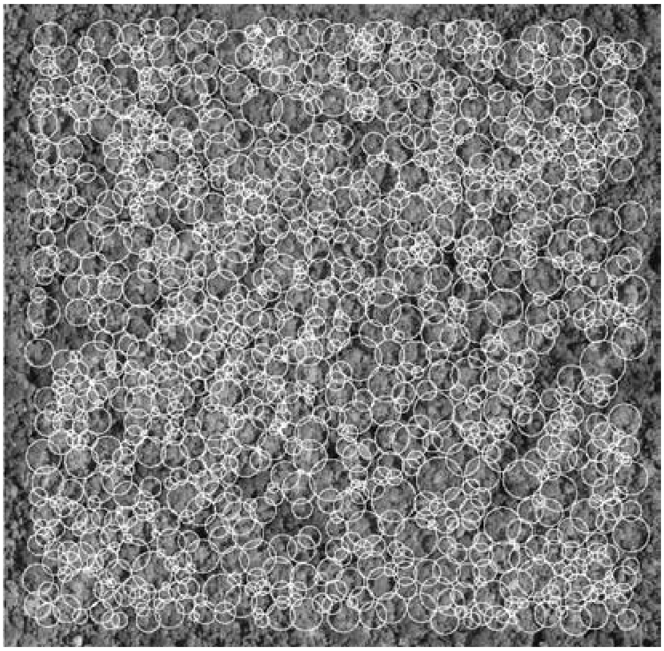

FIGURE 4. Sample output from crown detection algorithm. White circles represent crown edges. This is the same area as Figure 3.

CALIBRATION AT CAUAXI.—A calibration of the algorithm was performed on the parameters: (1) the derivative threshold and (2) the local maximum analysis range using data from 64 ha (800 × 800 m) of undisturbed forest at Cauaxi (Figs. 3 and 4). Crown size distributions (binned in 2-m classes) from our automated crown delineation algorithm were compared with field measurements from Asner *et al.* (2002). We measured goodness of fit using the root mean squared error of crown width distribution to identify algorithm parameters that best simulated Cauaxi field data.

ANALYSIS AT TAPAJOS AND 51 OTHER LOCATIONS.—Following the calibration using data from Cauaxi, we analyzed an IKONOS image taken of the Tapajos National Forest in the central Brazilian Amazon. The local maximum analysis range is reset for each image analyzed, using the maximum and modal DN values determined in image preprocessing. The derivative threshold was unchanged through all analyses following the original calibration. We then compared the results from the Tapajos image analysis to field data (Keller *et al.* 2001).

STATISTICAL ANALYSIS.—Crown width and dbh variables from both field and automated estimates had significantly different variances as determined by *F*-tests (Sokal & Rolff 1995). Because of the differences in variances we tested for difference between means using Welch's approximate *t*-test of equality of the means of two samples whose variances are assumed to be unequal (Sokal & Rolff 1995). We also compared distributions of crown widths and dbh's using a Kolmogorov–Sminov two-sample test for testing the differences in distributions of two samples of continuous observations (Sokal & Rolff 1995). This nonparametric test with the null hypothesis that two distributions do not differ is sensitive to differences in central location, dispersion, and skewness. To estimate differences in forest structure among a variety of forest sites, we examined 51 IKONOS image subsets listed in Table S1. Comparisons of the results from geographic sites were done using an ANOVA with Tukey–Kramer HSD comparison ($\alpha = 0.05$).

RESULTS

CALIBRATION (CAUAXI).—Forest structural variables from the Cauaxi image analysis are presented in Table 1. The average estimated crown width was 12.7 ± 0.1 m (mean ± SE), with a minimum of 2 m and a maximum of 34 m. No significant differences were found between mean field-estimated crown widths (for both all trees and no understory) and our automated mean crown estimate using a Welch's approximate *t*-test, although the difference between distributions of crown widths for automated analysis versus field data (Fig. 5) was significant (Kolmogorov-Smirnov test; $P < 0.01$) regardless of whether we tested against all tree data or data for which the understory trees are excluded.

The frequency of trees detected at Cauaxi by the automated algorithm was 76.6/ha. Using the allometric relation between crown width and dbh (equation (1)), the mean dbh estimate from IKONOS was 54.0 ± 0.3 cm. Biomass estimated from the algorithm dbh and equation (2) was 262 Mg/ha. The tree areal frequency and biomass estimates compared well with field data (Tables 2 and 3). Using Welch's approximate *t*-test, we found no significant difference between mean field-estimated dbh for both the set of all trees ($t' = 0.86$) and the set with understory excluded ($t' = 0.57$). The automated algorithm provided better estimates of the mean crown width and mean dbh than that of manual crown delineation from Asner *et al.* (2002) (Table 1).

COMPARISON WITH TAPAJOS.—Although we lack actual field estimates of crown width at Tapajos, using field-estimated dbh we estimated crown width using data from Keller *et al.* (2001) and equation (1) of this paper. The automated algorithm estimated a mean crown width at Tapajos of 13.1 ± 0.1 m, with a minimum of 2 m and a maximum of 38 m (Table 1). No significant difference was identified between mean field-estimated crown width and our automated mean crown estimate ($t' = 0.04$), using Welch's approximate *t*-test (Table 1). Crown width distributions showed a significant difference between automated estimates and crown width estimates derived from field-measured dbh (Kolmogorov-Smirnov test; $P < 0.01$). The automated algorithm estimated the frequency of trees as 76.4 trees/ha, and the mean dbh as 55.8 ± 0.4 cm. The mean dbh estimate based on the automated analysis was also not significantly different from the field-measured values (Welch's approximate *t*-test; $t' = 0.14$). The automated estimate for aboveground biomass was 290 Mg/ha at Tapajos.

MULTI-SITE ANALYSIS.—Estimates of the mean (± SE) crown width, frequency of trees, dbh, and biomass derived from the automated crown detection algorithm on 51 IKONOS image subsets are

TABLE 1. *Crown characteristics derived from the automated crown detection algorithm for the Cauaxi and Tapajos forest stands. dbh estimates from automated crown detection algorithm and allometric equation (1).*

Cauaxi					Tapajos		
Crown width (m)	IKONOS	IKONOS	Field Data	Field Data	Crown Width (m)	IKONOS	Field Data
Quantiles	Automated	Manual*	No Understory*	All*	Quantiles	Automated	Derived from***
Maximum	34	40	41	41	Maximum	38	30
Upper quartile	16	20	15	13	Upper quartile	18	15
Median	12	16	11	9	Median	12	13
Lower quartile	8	10	8	7	Lower quartile	8	11
Minimum	2	3	1	1	Minimum	2	6
Crown Width	IKONOS	IKONOS	Field data	Field data	Crown width	IKONOS	Field data
Moments	Automated	Manual*	No Understory*	All*	Moments	Automated	All
Mean	13	16	12	11	Mean	13	13
Std Dev	6	8	2	2	SD	6	3
N	3972	1675	1370	2127	*N*	3963	5869
Cauaxi					Tapajos		
dbh (cm)	IKONOS		Field Data	Field Data	dbh (cm)	IKONOS	Field Data
Quantiles	Automated		No Understory*	All*	Quantiles	Automated	All**
Maximum	138.7		172.0	172	Maximum	159.0	190.0
Upper quartile	66.1		53.0	44	Upper quartile	69.7	59.6
Median	52.3		37.0	30	Median	52.2	47.0
Lower quartile	39.6		26.0	23.8	Lower quartile	39.6	39.6
Minimum	22.9		20.0	20	Minimum	22.9	15.0
dbh	IKONOS		Field Data	Field Data	dbh	IKONOS	Field Data
Moments	Automated		No Understory	All	Moments	Automated	All
Mean	54.0		43.1	37.4	Mean	55.8	51.9
SD	19.0		3.6	3.4	SD	22.1	16.9
N	3972		1370	2127	*N*	3963	5869

*Cauaxi field data and manual interpretation are from Asner *et al.* (2002a).

**Tapajos field data is from Keller *et al.* (2001).

***Tapajos crown width derived from Tapajos field data for dbh from Keller et al. (2001) and equation (1) from this paper.

presented in Table 3. The Jaru image had the largest estimated average crown width and dbh (15.6 ± 0.2 m and 65.0 ± 0.5 cm, respectively), whereas Manaus had the smallest of these two estimates (11.3 ± 0.1 m and 49.3 ± 0.5 cm, respectively). Manaus had the highest tree frequency (99 ± 3 trees/ha) and Jaru had the lowest (53 ± 2 trees/ha). Aboveground biomass was estimated to be lowest at Tapajos km 67 (258 ± 3 Mg/ha), whereas Caxiuana (281 mg/ha) and Jaru (281 ± 5 Mg/ha) were remarkably similar. Santarem km 83 (275 ± 5 Mg/ha) and Alta Floresta (275 ± 3 Mg/ha) also had similar biomass estimates. Biomass estimates showed less variation among sites than crown width, tree frequency, and dbh.

Overall, there was an inverse relationship between mean crown width and tree frequency. Manaus and Jaru had markedly different structural characteristics compared to all other sites (Table S2). Alta Floresta showed a significant difference in estimated crown width and average dbh from Jaru and the two Tapajos sites. Biomass was found to be significantly different only between Santarem km 67 and Manaus, and Santarem km 67 and Alta Floresta (ANOVA; $F = 8.0$, $P < 0.001$).

DISCUSSION

Our algorithm for automated characterization of tropical forest canopy properties combines local maximum filtering and local minima value-finding methods, with analysis of ordinal transect data radiating outward from a crown apex (local maximum). Our method differs from an earlier approach to canopy delineation developed for coniferous forests (Pouliot *et al.* 2002) because we use a derivative threshold to end ordinal transect length instead of a regression analysis. Using the derivative threshold allowed us to analyze varied crown shapes, sizes, and spacing inherent in old-growth tropical forests. Iterative local maximum filtering allows for more of the canopy trees in an image to be examined, since some canopy trees with variation in color and brightness (due to leaf

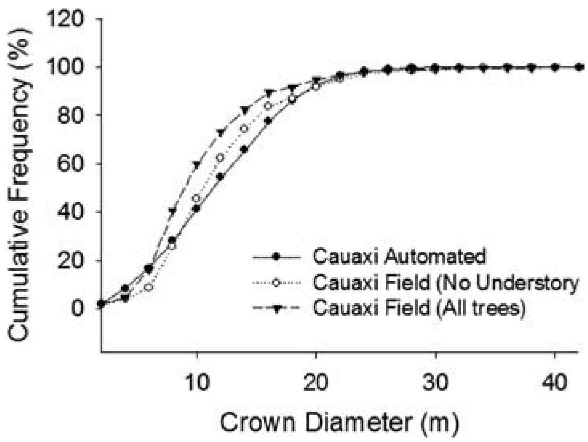

FIGURE 5. Cumulative frequency distribution for field-observed canopy diameters and automated crown estimate at Cauaxi.

phenology and flowering) might overwhelm a single local maximum analysis.

Our algorithm directly estimated crown widths and areal frequency (trees/ha) from the IKONOS satellite imagery. At both Cauaxi and Tapajos, the remotely sensed average crown widths were about 3 percent smaller than crown widths measured in the field (Table 1), and the differences between the means were not significant. Mean field-estimated crown width that excludes understory trees, matched even more closely with automated crown detection algorithm (Table 1). Although means were indistinguishable, significant differences in distributions were detected by the powerful Kolmogorov–Smirnov test. Comparison of our automated analysis with field data suggests that our algorithm tends to merge crowns leading to an excess of large trees. Lianas may lead to merged crowns as detected by our automated crown detection algorithm if they extend across more than one tree canopy (Avalos & Mulkey 1999). We have observed lianas extending over multiple smaller canopies from our own observations from towers above the canopy at the Tapajos forest. Interestingly, our automated algorithm provided better estimates of the mean crown width and mean dbh than that of manual crown delineation from Asner *et al.* (2002) (Table 1). Possibly, human observers are more prone to merge crowns than the automated algorithm. Considering the complexity of tropical forest structure and the inability to view understory trees in IKONOS image data, our algorithm compared well with field crown width data (Table 2).

At Cauaxi, field-measured stem frequency was 55 trees/ha for trees > 35 cm dbh and 137 trees/ha for trees > 20 cm dbh. Our detection algorithm identified 77 trees/ha, whereas manual interpretation of the same IKONOS image (Asner *et al.* 2002) yielded 47 trees/ha. Field-measured stem frequency at Tapajos ranged from 44 to 55 trees/ha for trees > 35 cm dbh to 168 trees/ha for trees > 15 cm dbh (Table 1), whereas the automated crown detection algorithm counted 76 trees/ha at that site. Clearly, the automated crown detection algorithm is unable to count understory trees; the algorithm measured stem frequency with an apparent cut-off diameter near 28 cm, based on the number of trees (76) per hectare found through filtering field data. Aboveground biomass was estimated via two allometric equations: (1) crown width to dbh from fieldwork done at Cauaxi; and (2) dbh to biomass (Brown 1997), and is thus subject to compounded errors. Field-estimated aboveground biomass at Cauaxi was 249 Mg/ha for trees greater then 20 cm dbh, whereas biomass estimated using automated crown detection algorithm was only 5 percent higher (Table 1). Greater biomass estimates from the automated processing routine may be biased high because of the tendency for the algorithm to merge crowns.

An examination of 51 (1 km^2) areas from seven LBA sites located throughout the Amazon showed considerable variation in crown width, dbh distribution, and stem frequency although estimates of biomass were relatively constant. Analysis of variance showed that crown widths at Jaru and Manaus differed from all other sites as well as with each other. Forest stands converged to similar biomass despite differences in structural parameters such as tree frequency and crown width (Table 2). The similarity of biomass across sites results from a trade-off of stem frequency and maximum tree sizes. We note that we made no attempt to adjust our biomass estimates for wood density as has been suggested by recent studies (Baker *et al.* 2004), and we acknowledge the preliminary nature of our estimates. In addition, if we had selected alternative allometries

TABLE 2. *Remotely sensed estimates and field data of stand density and biomass from Cauaxi and Tapajos in the Brazilian Amazon.*

Source	Site	Size of survey (ha)	Density (trees/ha)	Biomass (mg/ha)
Keller *et al.* (2001)	Tapajos km 83 (1997)	392	55 > 35 cm dbh	177 > 35 cm dbh
			168 > 15 cm dbh[1]	224 > 15 cm dbh [1]
Rice *et al.* (2004)	Tapajos km 67 (2001)	4	496 > 10 cm dbh	311.0 > 10 cm dbh
	Tapajos km 67 (2001)	20	43.8 > 35 cm dbh	193.3 > 35 cm dbh
Field Data 2	Cauaxi (2000)	15.8	137.27 >20 cm dbh	248.97 > 20 cm dbh
	Cauaxi (2000)	15.8	55.1 > 35 cm dbh	202.8 > 35 cm dbh
Automated estimate	Cauaxi	51.8	76.6	262
Automated estimate	Tapajos	51.8	76.4	290.4

[1]Trees < 35 cm dbh were not measured by Keller *et al.* (2001) but were modeled using the de Liocourt quotient.

[2]Based on data presented in Asner *et al.* (2002).

TABLE 3. *Results from automated algorithm run on IKONOS image data at different LBA sites throughout the Brazilian Amazon.*

Site name	IKONOS Tiles	Average crown width (m) Mean	SE	Average dbh (cm) Mean	SE	Biomass (Mg/ha) Mean	SE	Areal frequency (number/ha) Mean	SE
Cauaxi	14	13.3	0.1	56.4	0.4	266	2	70	1
Caxiuana	1	12.3		53.1		281		83	
Jaru	2	15.6	0.2	65.0	0.5	281	5	53	2
Manaus	9	11.3	0.1	49.3	0.5	279	2	99	3
Alta Floresta	10	13.0	0.2	55.2	1.0	275	2	76	2
Santarem 67	10	13.8	0.1	57.9	0.5	258	3	65	2
Santarem 83	5	13.7	0.3	58.0	0.8	275	5	68	3

specific to the Central Amazon (*e.g.*, Chambers *et al.* 2001) or applicable across tropical moist forests (Chave *et al.* 2005), we would get slightly different estimates (Keller *et al.* 2001), but the general pattern of similar biomass across sites would remain.

Comprehensive validation data do not exist for most of the sites that we analyzed because forest structure data are rare across the Amazon. However, we note that our estimates for Tapajos and Manaus show trends that are similar to field data collected by Vieira *et al.* (2004), who found 164 trees/ha > 25 cm dbh in plots outside of Manaus and only 104 trees/ha > 25 cm dbh in plots at the Tapajos National Forest. These findings, while not proof, are a positive indication that our technique may be useful for diagnosing structural properties of large areas of remote tropical forests where ground-based data are scarce.

Crown width is an important variable that we examined using high spatial resolution satellite imagery, and the distributions of crown widths may be a useful indicator for forest disturbance regimes or successional state. The frequency of gap-phase disturbance is a key regulator of forest dynamics in the lowland tropics (West *et al.* 1981; Brokaw 1985, 1987; Denslow 1987; Svenning 2000). Forests structure is directly tied to various types of disturbance, which function on different spatial and temporal scales. For example, the presence of very large crown diameters may indicate long periods between catastrophic disturbances. Forests experiencing small-scale disturbances from the deaths of individual trees are likely to have different crown width distributions than forests that have experienced large-scale disturbances, such as blow-downs.

It is difficult to estimate Amazonian biomass mainly because of the limited areas sampled and potential biases in ground surveys (Houghton *et al.* 2000; Keller *et al.* 2001). Knowledge of Amazonian biomass is vital to estimates of carbon stocks and fluxes for this globally important forest region. Our automated crown characterization program could be used in coordination with ground surveys and other data to randomly sample large areas and develop estimates of biomass and other aspects of forest structure for remote areas of Amazonia.

CONCLUSIONS.—We developed and tested an automated algorithm that uses high spatial resolution imagery with a combination of techniques for characterization of landscape-level canopy properties. This remote sensing method is a first step toward automated analysis of crown width distributions and stem frequency using high spatial resolution panchromatic imagery from IKONOS over remote tropical forest ecosystems. Remotely sensed average crown widths were within 3 percent of the crown widths derived from field measurements and were not significantly different from field-measured means. Using allometric relations, we have estimated dbh distributions and biomass of these forests. We found that the remotely sensed crown width and dbh distributions were incapable of detecting small understory trees and overestimated the size and frequency of large trees. These errors are probably caused by an inability to view smaller understory trees, merging of smaller tree crowns, and lianas bridging tree crowns. High spatial resolution satellite data are increasingly available and should be available in the future because of commercial and government demands for these products. With such data, it is now possible to randomly sample large areas and develop estimates of forest structure for regions such as the Amazon basin. Furthermore, the commercial market for high spatial resolution satellite image products will facilitate data access providing temporal and spatial coverage for further analysis and survey work.

ACKNOWLEDGMENTS

We thank J. Zweede, R. Pereira Jr. and the foresters and technicians of the Fundacao Floresta Tropical (FFT) for their support of this project. Funding for this research was provided by the USDA Forest Service, the NASA Terrestrial Ecology Program (NCC5−225), and the NASA New Millenium Program (NCC5–481).

SUPPLEMENTARY MATERIAL

The following supplementary material for this article is available online at: www.blackwell-synergy.com/loi/btp

Table S1. *Center coordinates of each 1 × 1 km IKONOS image subset used in the analysis.*

Table S2. *Comparisons of crown detection algorithm results between different LBA forest sites using ANOVA.*

LITERATURE CITED

Asner, G. P., and A. S. Warner. 2003. Canopy shadow in IKONOS satellite observations of tropical forests and savannas. Remote Sens. Environ. 87: 521–533.

Asner, G. P., D. E. Knapp, E. N. Broadbent, P. J. C. Oliveira, M. Keller, and J. N. Silva. 2005. Selective logging in the Brazilian Amazon. Science 310: 480–482.

Asner, G. P., M. Palace, M. Keller, R. Pereira, J. N. M. Silva, and C. Zweede. 2002. Estimation canopy structure in an Amazon forest from laser range finder and IKONOS satellite observations. Biotropica 34: 483–492.

Avalos, G., and S. S. Mulkey. 1999. Seasonal changes in liana cover in the upper canopy of a Neotropical dry forest. Biotropica 3: 186–192.

Baker, T. R., O. L. Phillips, Y. Malhi, S. Almeida, L. Arroyo, A. Di Fiore, T. Erwin, T. J. Killeen, S. G. Laurance, W. F. Laurance, S. L. Lewis, J. Lloyd, A. Monteagudo, D. A. Neill, S. Patino, N. C. A. Pitman, J. N. Silva, and R. V. Martinez. 2004. Variation in wood density determines spatial patterns in Amazonian forest biomass. Global Change Biol. 105: 545–562.

Bolduc, P., K. Lowell, and G. Edwards. 1999. Automated estimation of localized forest volume from large-scale aerial photographs and ancillary cartographic information in a boreal forest. Int. J. Remote Sens. 2018: 3611–3624.

Brandtberg, T., and F. Walter. 1998. Automated delineation of individual tree crowns in high spatial resolution aerial images by multiple-scale analysis. Mach. Vision Appl. 11: 64–73.

Brokaw, N. L. 1985. Gap-phase regeneration in a tropical forest. Ecology 6630: 682–687.

Brokaw, N. L. 1987. Gap-phase regeneration of three pioneer tree species in a tropical forest. J. Ecol. 75: 9–19.

Brown, S. 1997. Estimating biomass and biomass change of tropical forests: A primer. United Nations Food and Agriculture Organization.

Brown, S., T. Pearson, D. Slaymaker, S. Ambagis, N. Moore, D. Novelo, and W. Sabido. 2005. Creating a virtual tropical forest from three-dimensional aerial imagery: Application for estimating carbon stocks. Ecol. Appl. 15: 1083–1095.

Caelli, T., L. Cheng, and Q. Fang. 2005. Bayesian image understanding: From images to virtual forests. Int. J. Robotics Automation 20: 14–24.

Chambers, J. Q., J. Santos, R. J. Ribeiro, and N. Higuchi. 2001. Tree damage, allometric relationships, and above-ground net primary production in a tropical forest. For. Ecol. Manage. 152:73–84.

Chave, J., B. Riera, and M. A. Dubois. 2001. Estimation of biomass in a Neotropical forest of French Guiana: Spatial and temporal variability. J. Trop. Ecol. 17: 79–96.

Chen, Q., D. Baldocchi, P. Gong, and M. Kelly. 2006. Isolating individual trees in a Savanna woodland using small footprint lidar data. Photogramm. Eng. Remote Sens. 72: 923–932.

Cheng, L., T. Caelli, and A. Sanchez-Azofeifa. 2006. Component optimization for image understanding: A Bayesian approach. IEEE T. Pattern Anal. 28: 984–993.

Chubey, M. S., S. E. Franklin, and M. A. Wulder. 2006. Object-based analysis of Ikonos-2 imagery for extraction of forest inventory parameters. Photogramm. Eng. Remote Sens. 72: 383–394.

Clark, D. B., C. S. Castro, L. D. A. Alvarado, and J. M. Read. 2004. Quantifying mortality of tropical rain forest trees using high-spatial-resolution satellite data. Ecol. Lett. 7: 52–59.

Culvenor, D. S. 2002. TIDA: An algorithm for the delineation of tree crowns in high spatial resolution remotely sensed imagery. Computers Geosci. 28: 33–44.

Dawkins, H. C. 1962. Crown diameters: Their relation to bole diameter in tropical forest trees. Commonw. Forest. Rev. 26: 318–333.

Denslow, J. S. 1980. Gap partitioning among tropical rainforest trees. Tropical Succession 12: 47–77.

Denslow, J. S. 1987. Tropical rainforest gaps and tree species diversity. Annu. Rev. Ecol. Syst. 18: 431–451.

Falkowski, M. J., A. M. S. Smith, A. T. Hudak, P. E. Gessler, L. A. Vierling, and N. L. Crookston. 2006. Automated estimation of individual conifer tree height and crown diameter via two-dimensional spatial wavelet analysis of lidar data. Can. J. Remote Sens. 32: 153–161.

Fensham, R. J., R. J. Fairfax, J. E. Holman, and P. J. Whitehead. 2002. Quantitative assessment of vegetation structural attributes from aerial photography. Int. J. Remote Sens. 2311: 2293–2317.

Gong, P., Y. Sheng, and G. S. Biging. 2002. 3D Model-based tree measurement from high-resolution aerial imagery. Photogrammetric Engineering & Remote Sensing 68:203–1212.

Gougeon, F. A. 1995a. A crown-following approach to the automatic delineation of individual tree crowns in high spatial resolution aerial images. Can. J. Remote Sens. 21: 274–284.

Gougeon, F. A. 1995b. Comparison of possible multispectral classification schemes for tree crowns individually delineated on high spatial resolution MEIS Images. Can. J. Remote Sens. 21: 1–9.

Houghton, R. A., K. T. Lawrence, J. L. Hackler, and S. Brown. 2001. The spatial distribution of forest biomass in the Brazilian Amazon: A comparison of estimates. Global Change Biol. 7: 731–746.

Houghton, R. A., D. L. Skole, C. A. Nobre, J. L. Hackler, K. T. Lawrence, and W.H. Chomentowski. 2000. Annual fluxes of carbon from the deforestation and regrowth in the Brazilian Amazon. Nature 403: 301–304.

Hurtt, G., X. Xiao, M. Keller, M. Palace, G. P. Asner, R. Braswell, E. S. Brondizio, Manoel Cardoso, C. J. R. Carvalho, M. G. Fearon, L. Guild, S. Hagen, T. Sá, A. Schloss, G. Vourlitis, A. J. Wickel, B. Moore III, and C. Nobre. 2003. IKONOS imagery for the large scale biosphere—atmosphere experiment in Amazonia LBA. Remote Sens. Environ. 88: 111–127.

Jensen, O. C., and A. Sanchez Azofeifa. 2006. Satellite-derived ecosystems classification: Image segmentation by ecological region for improved classification accuracy, a boreal case study. Int. J. Remote Sens. 27: 233–251.

Keller, M., A. Alencar, G. P. Asner, B. Braswell, M. Bustamante, E. Davidson, T. Feldpausch, E. Fernandes, M.Goulden, P. Kabat, B. Kruijt, F. Luizão, S. Miller, D. Markewitz, A.D. Nobre, C. A. Nobre, N. Priante Filho, H. Rocha, P. Silva Dias, C. von Randow, and G. L. Vourlitis. 2004. Ecological research in the large scale biosphere atmosphere experiment in Amazônia LBA: early results. Ecol. Appl. 14: S3–S16.

Keller, M., M. Palace, and G. Hurtt. 2001. Biomass estimation in the Tapajos National Forest, Brazil. Estimation of sampling and allometric uncertainties. For. Ecol. Manage. 154: 371–382.

Larsen, M., and M. Rudemo. 1988. Optimizing templates for finding trees in aerial photographs. Pattern Recog. Lett. 19: 1153–1162.

Leckie, D. G., F. A. Gougeon, D. Hill, R. Quinn, L. Armstrong, and R. Shreenan. 2003a. Combined high density lidar and multispectral imagery for individual tree crown analysis. Can. J. of Remote Sens. 29: 1–17.

Leckie, D. G., F. A. Gougeon, S. Tinis, T. Nelson, C. N. Burnet, and D. Paradine. 2005a. Automated tree recognition in old growth conifer stands with high resolution digital imagery. Remote Sens. Environ. 94: 311–326.

Leckie, D. G., F. A. Gougeon, N. Walsworth, and D. Paradine. 2003b. Stand delineation and composition estimation using semi-automated individual tree crown analysis. Remote Sens. Environ. 85: 355–369.

Leckie, D. G., S. Tinis, T. Nelson, C. N. Burnet, F. A. Gougeon, E. Cloney, and D. Paradine. 2005b. Issues in species classification of trees in old growth conifer stands. Can. J. Remote Sens. 31: 175–190.

Moran, E. F., E. Brondizio, P. Mausel, and Y. Wu. 1994. Integrating Amazonian vegetation, land-use, and satellite data. Bioscience 44: 329–338.

Ozanne, C. M. P., D. Anhuf, S. L. Boulter, M. Keller, R. L. Kitching, C. Korner, F. C. Meinzer, A. W. Mitchell, T. Nakashizuma, P.

L. S. Dias, N. E. Stork, S. J. Wright, and M. Yoshimura. 2003. Biodiversity meets the atmosphere: A global view of forests canopies. Science 301: 183–186.

Popescu, S. C., R. H. Wynne, and R. F. Nelson. 2003. Measuring individual tree crown diameter with lidar and assessing its influence on estimating forest volume and biomass. Can. J. Remote Sens. 29: 564–577.

Pouliot, D. A., D. J. King, F. W. Bell, and D. G. Pitt. 2002. Automated tree crown detection and delineation in high-resolution digital camera imagery of coniferous forest regeneration. Remote Sens. Environ. 82: 322–334.

Quackenbush, L. J., P. F. Hopkins, and G. J. Kinn. 2000. Using template correlation to identify individual trees in high resolution imagery. American Society for Photogrammetry & Remote Sensing (ASPRS) 2000 Annual Conference Proceedings, Washington DC.

Read, J. M., D. B. Clark, E. M. Venticinque, and M. P. Moreira. 2003. Application of merged 1-m and 4-m resolution satellite data to research and management in tropical forests. J. Appl. Ecol. 40: 592–600.

Rice, A. H., E. H. Pyle, S. R. Saleska, L. Hutyra, P. B. Camargo, K. Portilho, D. F. Marques, M. Palace, M. Keller, and S. C. Wofsy. 2004. Carbon balance and vegetation dynamics in an old-growth Amazonian forest. Ecol. Appl. 144: s55-s71.

Richards, P. W. 1952. The tropical rain forest: An ecological study. Cambridge University Press, Cambridge, UK.

Roberts, D. A., M. Keller, and J. V. Soares. 2003. Studies of land-cover, land-use, and biophysical properties of vegetation in the large scale biosphere atmosphere experiment in Amazonia. Remote Sens. Environ. 87: 377–388.

Roughgarden, J., S. Running, and P. Matson. 1991. What does remote sensing do for ecology? Ecology 726: 1918–1922.

Salati, E., and P. B. Vose. 1984. Amazon basin: A system in equilibrium. Science 225: 129–138.

Scarth, P., and S. Phinn. 2000. Determining forest structural attributes using an inverted geometric-optical model in mixed eucalypt forests, Southeast Queensland, Australia. Remote Sens. Environ. 71: 141–157.

Schwarzkopt, L., and A. B. Rylands. 1989. Primate species richness in relation to habitat structure in Amazonian rainforests fragments. Biol. Conserv. 48: 1–12.

Shugart, H. H., L. Bourgeau-Chavez, and E. S. Kasischke. 2001. Determination of stand properties in boreal and temperate forests using high-resolution imagery. For. Sci. 46: 478–486.

Skole, D., and C. Tucker. 1993. Tropical deforestation and habitat fragmentation in the Amazon: Satellite data from 1978 to 1988. Science 260: 1905–1910.

Sokal, R. R., and F. J. Rohlf. 1995. Biometry: the principles and practice of statistics *In* Biological Research. 3rd edn., W. H. Freeman and Co., New York, New York.

Souza, C., L. Firestone, L. M. Silva, and D. Roberts. 2003. Mapping forest degradation in the Eastern Amazon from SPOT 4 through spectral mixture models. Remote Sens. Environ. 87: 494–506.

Spies, T. A. 1998. Forest Structure: A key to the ecosystem. *In* J. A. Trofymow and A. MacKinnon (Eds.). Proceedings of a workshop on Structure, Process, and Diversity in Successional Forests of Coastal British Columbia, February 17–19, 1998, Victoria, British Columbia. Northwest Science, Vol. 72 (special issue No. 2), pp. 34–39.

Steininger, M. 1996. Tropical secondary forest regrowth in the Amazon: Age, area, and change estimation with Thematic Mapper. Int. J. Remote Sens. 171: 9–2.

Stiteler, W. M., and P. F. Hopkins. 2000. Using genetic algorithms to select tree crown templates for finding trees in digital imagery. American Society for Photogrammetry & Remote Sensing (ASPRS) 2000 Annual Conference Proceedings, Washington DC.

Svenning, J. C. 2000. Small canopy gaps influence plant distributions in the rain forest understory. Biotropica 322: 252–261.

Terborgh, J. 1992. Maintenance of diversity in tropical forests. Biotropica 24: 283–292.

Terborgh, J., R. B. Foster, and P. Nunez. 1996. Tropical tree communities: A test of the nonequilibrium hypothesis. Ecology 77: 561–567.

Vieira, S., P. B. Camargo, D. Selhorst, R. Silva, L. Hutyra, J. Q. Chambers, I. F. Brown, N. Higuchi, J. Santos, S. Wofsy, S. E. Trumbore, and L. A. Martinelli. 2004. Forest structure and carbon dynamics in Amazonian tropical rain forest. Oecologia 40: 468–479.

Weinacker, H., B. Koch, U. Heyder, and R. Weinacker. 2004. Development of filtering, segmentation and modelling modules for lidar and multispectral data as a fundament of an automatic forest inventory system. International Society Of Photogrammetry And Remote Sensing. *In* M. Thies, B. Koch, H. Spiecker, and H. Weinacker (Eds.). Proceedings of the ISPRS working group VIII/2, Laser-Scanners for Forest and Landscape Assessment, Freiburg, Germany 03–06 October 2004.

West, D. C., H. H. Shugart, and D. B. Botkin. 1981. Forest succession. Concepts and application. Springer-Verlag, New York, New York.

Whitmore, T. C. 1982. On pattern and process in forests. *In* E. I. Newman (Ed.). The plant community as a working mechanism, pp. 45–59 Blackwell Scientific Publications, Oxford, UK.

Wulder, M., K. O. Niemann, and D. G. Goodenough. 2000. Local maximum filtering for the extraction of tree locations and basal area from high spatial resolution imagery. Remote Sens. Environ. 73: 103–114.